Biomaterials 33 (2012) 4646–4652

Contents lists available at SciVerse ScienceDirect

Biomaterials

journal homepage: www.elsevier.com/locate/biomaterials

Sustained release of proteins from high water content supramolecular polymer hydrogels

Eric A. Appel [a], Xian Jun Loh [a], Samuel T. Jones [a], Cecile A. Dreiss [b], Oren A. Scherman [a,*]

[a] Melville Laboratory for Polymer Synthesis, Department of Chemistry, Cambridge University, Lensfield Road, Cambridge CB2 1EW, UK[1]
[b] Institute of Pharmaceutical Science, King's College London, Franklin-Wilkins Building, 150 Stamford Street, London SE1 9NH, UK

ARTICLE INFO

Article history:
Received 30 January 2012
Accepted 14 February 2012
Available online 27 March 2012

Keywords:
Controlled drug release
Drug release
Growth factors
Hydrogel
Polyvinylalcohol
Cellulose

ABSTRACT

Self-assembled hydrogels with extremely high water content (up to 99.5%) and highly tunable mechanical properties were prepared from renewable cellulose derivatives. These hydrogels are easily processed and the simplicity of their preparation, their availability from inexpensive renewable resources, and the tunability of their mechanical properties are distinguishing for important biomedical applications. The protein release characteristics were investigated to determine the effect of both the protein molecular weight and polymer loadings of the hydrogels on the protein release rate. Extremely sustained release of bovine serum albumin is observed over the course of 160 days from supramolecular hydrogels containing only 1.5 wt% polymeric constituents. This sustained release far surpasses the current state of the art for protein release from a hydrogel, highlighting these materials as important potential candidates for sustained therapeutic applications.

© 2012 Elsevier Ltd. All rights reserved.

1. Introduction

Protein therapeutics have demonstrated many advantages over small-molecule drugs (a) by performing highly specific and complex functions, (b) decreasing the potential to interfere with normal biological processes, (c) lowering immune response, (d) generally resulting in faster clinical development and FDA approval time, (e) and providing facile and far-reaching patent protection of on account of their highly unique form and function [1]. These advantages make the development of protein therapeutics an extremely fast growing area and they have therefore had a significant role in almost every field of medicine. Recent advances in protein therapeutics, including antibodies which combat the spread of human immunodeficiency virus (HIV) [2,3], highlight the need for controlled delivery as a part of an effective treatment. The importance of sustained release is especially necessary in treatment of entire populations which have a high incidence of infectious diseases that do not currently have cures/vaccines. In these cases, entire populations can be dependent on every symptomatic and asymptomatic carrier of a chronic infection to take a medication on a regular basis (daily, weekly, etc.) in order to halt the spread of infection. Indeed patient compliance in pharmacologically therapeutic regimes, especially in asymptomatic patients, stops after only 6 months, causing enormous problems in the long term treatment of pandemic exposure to such infections [4]. Sustained release of such protein therapeutics from an injectable hydrogel, requiring an injection only periodically, has the potential to dramatically affect, and perhaps halt entirely, such pandemics by coupling highly effective therapeutics with a delivery system that limits the dependence of the population on each individual patient compliance.

Hydrogels are a type of biomaterial which have shown themselves to be particularly important candidates for drug delivery and tissue engineering applications given their similarity to soft biological tissue and highly variable mechanical properties [5–7]. Several systems exist, which have been thoroughly studied for their sustained drug release properties for drug delivery applications, wound covering and chemosensensitizing for cancer therapy [8–13]. A high concentration of the polymeric constituents is often needed in these formulations, sometimes requiring greater than 15 wt%, and many times such formulations exhibit poor resilience and strong 'burst' release of drugs. Indeed it has been traditionally observed that direct encapsulation of protein therapeutics into hydrogels exhibit a rapid 'burst' release during the initial swelling phase, followed by an extended, diffusion-controlled release of the protein, which was retarded by the hydrogel network [14]. It has even been suggested that the controlled release of protein over a long time is entirely unexpected because of the diffusion-controlled nature through aqueous channels within the hydrogel

* Corresponding author. Tel.: +44 1223 331508.
E-mail address: oas23@cam.ac.uk (O.A. Scherman).
[1] Fax: +44 (0)1223 334866.

0142-9612/$ – see front matter © 2012 Elsevier Ltd. All rights reserved.
doi:10.1016/j.biomaterials.2012.02.030

network [15]. These shortcomings have made many of these systems unsuitable for many biomedical applications [16,17]. Recently, thermogelling polymers based on poly(PEG/PPG/PHB urethane)s requiring relatively low polymer concentrations (2 wt%) to form hydrogels from aqueous solutions upon heating have been described and shown promise for the direct encapsulation of proteins [18]. Moreover, the hydrolytic degradability of these triblock copolymers allowed for tunability of protein release, which was shown to extend up to approximately 75 days *in vitro* [12].

Recently, our laboratory has prepared extremely high water content (up to 99.75% water), self-assembled polymeric hydrogels based on the strong and highly specific hetero-ternary complex formation of the macrocyclic host cucurbit[8]uril (CB[8]) [19]. Cucurbit[*n*]uril ($n = 5-8, 10$; CB[*n*]) are a family of macrocyclic host molecules, which are methylene-linked oligomers of glycoluril that have a symmetric 'barrel' shape with two identical portal regions laced by ureido-carbonyl oxygens. The number of glycoluril units determines the size of the cucurbituril cavity without affecting the height of the molecular container (approximately 0.9 nm), similar to the CD family. While smaller homologues of the cucurbit[*n*]uril family (*i.e.* CB[5], CB[6] and CB[7]) are capable of binding single guests (typically cationic amines, metal or imidazolium ions) [20–23], CB[8] has a larger cavity volume and can simultaneously accommodate two guests (Fig. 1a) [24]. An electron-deficient first guest such as viologen (MV) and an electron-rich second guest such as a naphthyl moiety (Np) form a stable 1:1:1 ternary complex with CB[8] through multiple noncovalent interactions acting synergistically, resulting in exceptionally high equilibrium binding affinities ($K_a \leq 10^{14}$ M^{-2}) [25]. High water content hydrogels are formed primarily from naturally renewable cellulose derivatives which have been functionalized with a Np moiety (HEC-Np) upon the addition of a poly(vinyl alcohol) polymer modified with MV (PVA-MV) and CB[8]. The exceptionally low polymer concentration and high water content of this gel, along with the ease and mild conditions required for hydrogel preparation, makes it highly attractive for biomedical applications due to improved biocompatibility. Herein we report the encapsulation of several model protein therapeutics, bovine serum albumin (BSA) and lysozyme, within the hydrogel and their subsequent, sustained release *in vitro* (Fig. 1b). Bioactivity of the proteins upon release from the hydrogels and *in vitro* toxicity studies of these self-assembled hydrogels are also reported.

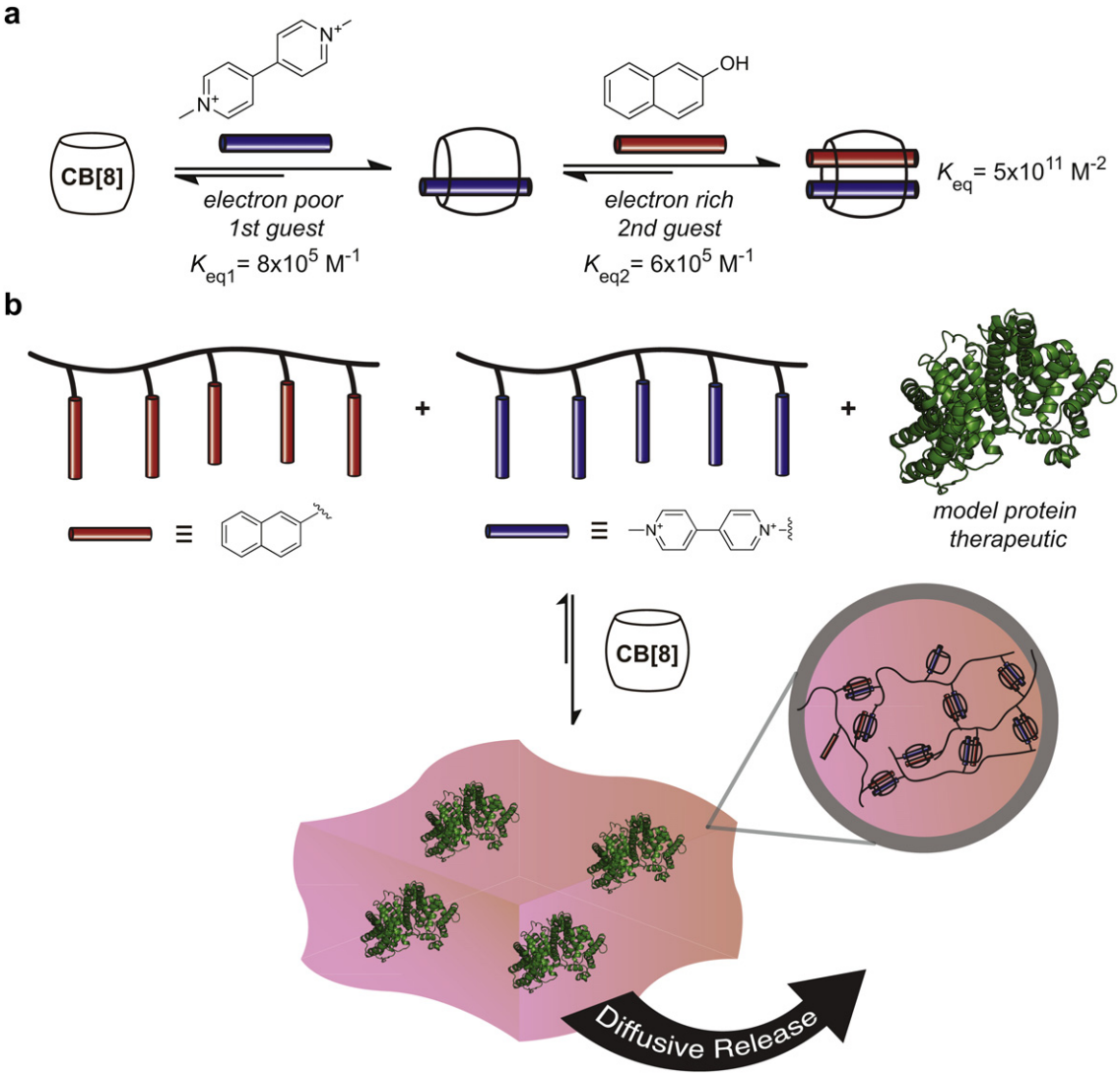

Fig. 1. a, Two-step, three-component binding of cucurbit[8]uril (CB[8]) in water. b, Schematic representation of the preparation of extremely high water content hydrogels through strong host–guest interactions of CB[8].

2. Experimental methods

2.1. Materials and methods

^{1}H NMR (400 MHz) spectra was recorded using a Bruker Avance QNP 400. Chemical shifts are recorded in ppm (δ) in D_2O with the internal reference set to δ 4.79 ppm. ATR FT-IR spectroscopy was performed using a Perkin–Elmer Spectrum 100 series FT-IR spectrometer equipped with a universal ATR sampling accessory. UV–VIS studies were performed on a Varian Cary 4000 UV–Vis spectrophotometer. Gel permeation chromatography (GPC) was carried out in water (H_2O) on a Shodex glucose column with a Shimadzu SPD-M20A prominence diode array detector, Optilab refractive index detector and dynamic light scattering detector (both Wyatt). Samples were filtered over 0.2 μm PVDF filters before injection using a 0.6 mL/min flow rate.

ITC titration experiments were carried out on a VP-ITC from Microcal Inc. at 25 °C in 10 mM sodium phosphate buffer (pH = 7). In a typical experiment, the host was in the sample cell at a concentration of 0.1 mM, and the guest was in the syringe at a 10 fold higher concentration. In the case of functional polymers, the concentration used is determined from the concentration of functional monomer units in solution and not the concentration of polymer. A titration consisted of 29 consecutive injections of 2–10 μL with at least 300 s intervals between injections. The first data point was removed from the data set prior to curve fitting. Heat of dilutions were checked by titration well beyond saturation or by titration of the guest into a buffer solution and subtracted from the normalized enthalpies, but relatively small in all cases. The data were analyzed with Origin 7.0 software, using the one set of sites model.

Rheological characterization was performed using an ARES-LC controlled strain rheometer fitted with a water bath set to 25 °C. Dynamic oscillatory strain amplitude sweep measurements were conducted at a frequency of 10 rad/s. Dynamic oscillatory frequency sweep measurements were conducted at a 5% strain amplitude. All measurements were performed using a 25 mm parallel plate geometry with a gap of 0.75 mm and analyzed using TA Instruments TA Orchestrator software.

Small-angle neutron scattering measurements were performed on D11 at the Institut Laue Langevin (ILL) (Grenoble, France). A wavelength (λ) of 10 Å and either two (or three) configurations were used to cover a q range from 4.4×10^{-3} Å^{-1} (or 6.8×10^{-4} Å^{-1}) to 3.1×10^{-1} Å^{-1}, where q is the modulus of the scattering vector. The samples were measured in 1 mm quartz cells using D_2O as a solvent and the data were recorded in a thermostatically controlled rack at 25 °C. The scattering from each sample was corrected for the electronic background, detector deadtime, scattering from the empty cell and sample transmission. The intensity was converted to the differential scattering cross-section in absolute units (cm^{-1}) using the scattering from a water sample. Data reduction was performed using the software Lamp, the Large Array Manipulation Program [26].

Scanning electron microscopy (SEM) images were obtained using a Leo 1530 variable pressure SEM using and InLens detector. SEM samples were prepared by direct freezing of the supramolecular hydrogels in liquid nitrogen followed by lyophilization. The resulting cryo-dried materials were imaged after sputtering.

Hydroxyethylcellulose (HEC) was purchased from Aldrich and dried overnight in a vacuum oven at 105 °C. Poly(vinylalcohol) (PVA, 98% hydrolyzed) was purchased from Aldrich, dissolved in water at 5 wt%, precipitated from a 1:1 solution of acetone and methanol, collected by suction filtration, and dried overnight at 60 °C. MV-NCO [27] and cucurbit[8]uril [28] were prepared according to a literature procedures. All other materials were purchased from Aldrich and used as received.

2.2. Synthesis of functional polymers

2.2.1. Synthesis of HEC-Np

HEC (1.00 g) was dissolved in *N*-methylpyrrolidone (NMP, 150 mL) at 110 °C. The solution was cooled to room temperature and Np-NCO (29.7 mg, 0.18 mmol) and dibutyltin dilaurate (TDL, 3 drops) were added and the mixture allowed to stir at room temperature overnight. The functional polymer was then purified by precipitation from acetone, filtered, and dried overnight under vaccum at 60 °C (1.01 g, 98%). ^{1}H NMR Spectroscopy (D_2O, 500 MHz) δ (ppm) = 7.99–7.29 (7H, br, Np-*H*), 4.60–2.75 (455H, br, cellulose backbone). Elemental: Found C, 47.14; H, 6.93; N, 0.68. $C_{85.5}H_{144.2}O_{60.6}N_1$ required C, 47.63; H, 6.74; N, 0.65. FT-IR (ATR) ν = 3410 (br), 2950 (br), 2910 (br), 1395, 1075 (s) cm^{-1}. GPC (H_2O): M_n (PDI) = 3.4 MDa (1.25).

2.2.2. Synthesis of PVA-MV

PVA (1 g) was dissolved in NMP (60 mL) and MV-NCO (0.63 g, 1.13 mmol) was added along with TDL (3 drops) and stirring overnight at room temperature. The functional polymer was then purified by precipitation from ethyl acetate, filtered, and dried overnight under vaccum at 60 °C (1.55 g, 95%). ^{1}H NMR Spectroscopy (D_2O, 500 MHz) δ (ppm) = 9.18–8.88 (4H, br, MV aryl-*H*), 8.60–8.33 (4H, br, MV aryl-*H*), 4.51–4.45 (2H, br, MV-CH_2), 4.38 (3H, s, MV-CH_3), 4.20–4.05 (3H, br, MV–CH_2–CH_2–OCN– and –NCO–CH from the backbone), 3.21–3.08 (4H, br, -CH_2-NCO-), 1.95–1.32 (48H, br, polymer backbone and hexamethylene linker). Elemental: Found C, 49.77; H, 7.66; N, 3.24. $C_{61}H_{106}O_{23}N_4B_2F_8$ required C, 50.98; H, 7.43; N, 3.90. FT-IR (ATR) ν = 3320 (br), 2920 (br), 2900 (br), 1715, 1690, 1580, 1450, 1290, 1060 (s), 820 cm^{-1}. GPC (H_2O): M_n (PDI) = 1.5 MDa (1.26).

2.3. Toxicity studies

Cells and media NIH 3T3 cells were cultivated in DMEM containing 10% fetal bovine serum (FBS) and 1% penicillin/streptomycin. Cells were grown as a monolayer and were passaged upon confluence using trypsin (0.5%, w/v in PBS). The cells were harvested from culture by incubating in trypsin solution for 10 min. The cells were centrifuged and the supernatant was discarded. Serum-supplemented DMEM (3 mL) was added to neutralize any residual trypsin. The cells were resuspended in serum-supplemented DMEM at a concentration of 2×10^4 cells/mL. Cells were cultivated at 37 °C and 5% CO_2.

The toxicities of the hydrogel constituent polymers were assessed by determining their ability to affect the proliferation and viability of 3T3 cells cultured in DMEM. The polymers were incubated in 24-well multiplates at 1×10^4 cells per well for 24 h at 37 °C in 500 μL of medium. The different cell viabilities were evaluated using the MTT assay on the 3T3 cell lines. Here, 10 mL of sterile filtered MTT stock solution in PBS (5 mg/mL) was added to each well, reaching a final MTT concentration of 0.5 mg/mL. After 5 h, unreacted dye was removed by aspiration. The formazan crystals were dissolved in DMSO (100 mL per well), and the absorbance was measured using a microplate reader at a wavelength of 570 nm. Cell viability (%) = $[A]_{test}/[A]_{control} \times 100\%$, where $[A]_{test}$ is the absorbance of the wells with polymers and $[A]_{control}$ is the absorbance of the control wells. All experiments were conducted with six repetitions and averaged. The control group consists of cells incubated without polymers and cultured in DMEM.

2.4. General preparation of self-assembled hydrogels

Hydrogels are prepared by first dissolving HEC-Np (5 mg) in water (0.5 mL) with stirring and mild heating. PVA-MV (0.1 mg) and CB[8] (0.1 mg) are then dissolved in water (0.5 mL) with some sonication (less than 5 min). The solutions are then mixed and shaken for approximately 1 s before hydrogel formation.

2.5. Protein release studies from hydrogels

Aqueous solutions of 1 and 3 wt% HEC-Np were mixed and left to equilibrate overnight at ambient temperature. Appropriate amounts of lysozyme or BSA solutions were loaded to a predetermined concentration of lysozyme or BSA in the polymer solution. Aqueous solution of PVA-MV (0.2 and 0.6 wt%) and CB[8] (0.2 and 0.6 wt%) were then prepared. In a typical example, 0.5 mL of protein-loaded HEC-Np polymer solution was injected into a sample vial and 0.5 mL of PVA-MV@CB[8] solution was added and the mixture shaken for approximately 1 s until the hydrogel formed. The sample vial was then placed in 7 mL of phosphate buffer release solutions in a test tube, which was incubated in a water bath equilibrated at 37 °C. The buffer solutions were replaced with fresh ones at predetermined time intervals, and the experiments were done in triplicate. The collected buffer solutions were lyophilized and kept at −80 °C for further analysis. The lysozyme and BSA contents were determined using the Pierce BCA Protein Assay kit. Quantification of lysozyme and BSA was based on a calibration curve, obtained using the fresh lysozyme and BSA standards, in the range of 20–2000 mg/mL [32].

2.6. Protein bioactivity studies

2.6.1. Activity of BSA

Esterase activity of BSA was determined by following the formation of para-nitrophenol from the synthetic substrate para-nitrophenyl acetate at 400 nm using a spectrophotometer. The reaction mixtures contained 50 μM p-nitrophenyl acetate and 20 μM protein in 0.1 M phosphate buffer, pH 7.4 at 37 °C. A molar extinction coefficient for para-nitrophenol of ε = 17,700 M^{-1} cm^{-1} was used for all the calculation.

2.6.2. Activity of lysozyme

Activity of the lysozyme released from the gel was determined using EnzChek® Lysozyme Assay Kit (Molecular Probes, E-22013). The experimental protocols were performed as per the instructions provided in the kit.

3. Results and discussion

3.1. High water content cellulose-based supramolecular hydrogels

3.1.1. Synthesis of functional polymeric precursors

A cellulose-based scaffold, hydroxyethyl cellulose (HEC), could be easily functionalized using commercially available 2-naphthyl isocyanate (Np) in a one-step reaction performed at ambient temperature in *N*-methylpyrrolidone using dibutyltin dilaurate (TDL) as a catalyst (Fig. 2a). Any excess isocyanate can be readily removed by precipitation of the naphthyl-functional cellulose (HEC-Np). This simple method is extendable to a variety of other

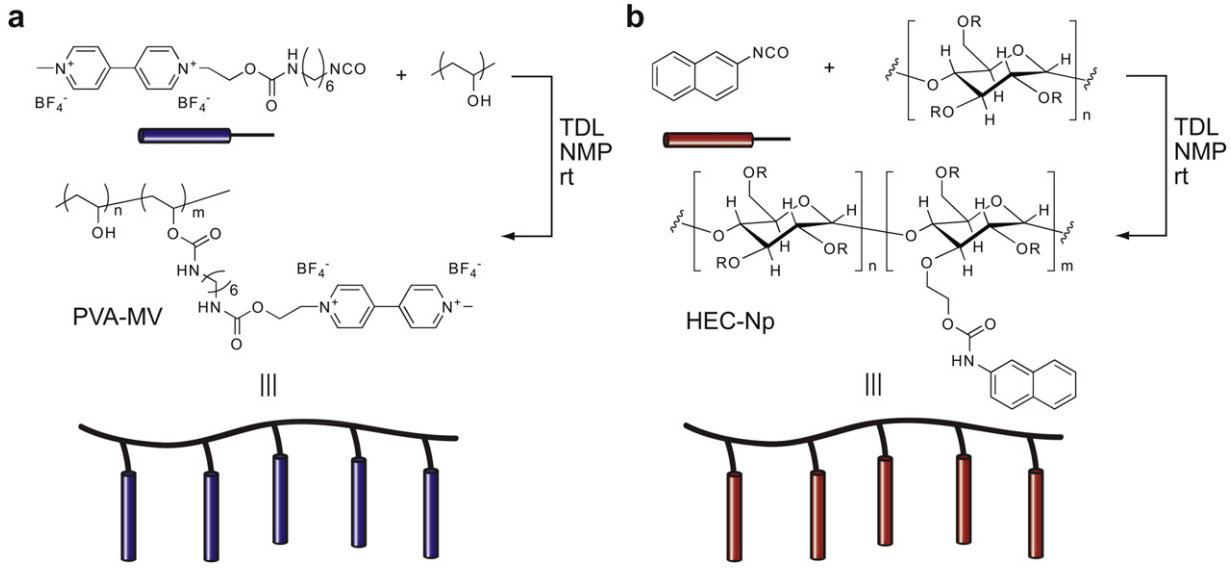

Fig. 2. Synthetic scheme for preparation of functional first guest (a) and second guest (b) precursors to self-assembled hydrogels.

isocyanate-functional second-guests which can be prepared by either employing diphenylphosphoryl azide (DPPA) [33] with carboxylic acids *via* thermal Curtius rearrangement, or reaction of triphosgene with amines [27]. Furthermore, a viologen unit containing a hydroxyl group can be reacted with an excess of 1,6-hexamethylene diisocyanate (HDI) to form the monofunctional addition product carrying one remaining isocyanate group for subsequent reaction yielding 1-(2-hydroxyethyl)-10-methyl-[4,40-bipyridine]-1,10-diium di(tetrafluoroborate) (MV-NCO). This moiety was conjugated to commercially available poly(vinyl alcohol) (PVA) using similar conditions as mentioned above to produce a viologen-functional polymer (PVA-MV, Fig. 2a). These synthetic protocols are facile, rapid and are easily scaled.

3.1.2. Preparation and characterization of self-assembled hydrogels

Simple mixing of a solution of HEC-Np (0.5 wt%) with a solution of PVA-MV (0.1 wt%) containing a 1:1 loading of MV:CB[8] (PVA-MV@CB[8]) instantaneously produced a lightly orange colored, transparent hydrogel. The orange color is inherent to the MV:Np:CB[8] ternary complex and is a product of the charge–transfer complex between the MV and Np moieties within the CB[8] cavity [25]. There is a clear dependence of hydrogel formation on the presence of all three components of the ternary complex as only the system with Np, MV and CB[8] forms hydrogels (Fig. 3). A lack of any one of the components, or the addition of CB[7] (whose cavity is only large enough to encapsulate MV alone) instead of CB[8] does not yield hydrogels.

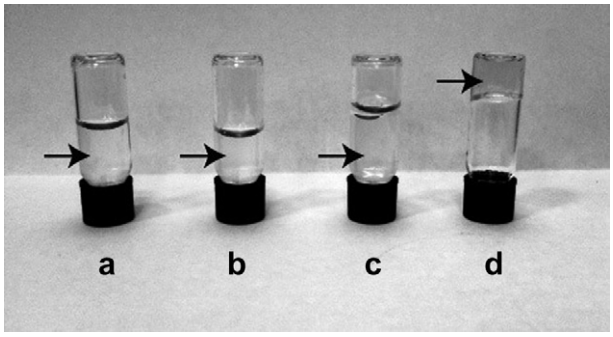

Fig. 3. Inverted vial test for the preparation of self-assembled hydrogels. a, HEC-Np 0.5 wt%. b, HEC-Np 0.5 wt%/PVA-MV 0.1 wt%. c, HEC-Np 0.5 wt%/PVA-MV 0.1 wt %/CB[7] 1eq. d, HEC-Np 0.5 wt%/PVA-MV 0.1 wt%/CB[8] 1eq.

The mechanical properties of the hydrogels were characterized with rheometric measurements. Strain dependent oscillatory rheology (Fig. 4a) displays an extremely broad linear viscoelastic region and it is only at higher loading (1.5 wt%) that a deviation from linear vicoelasticity is observed. The frequency dependence of the storage and loss oscillatory shear moduli (G' and G'', respectively), clearly identifies hydrogel-like behaviour as the two are linear and parallel and G' is dominant across the whole range of frequencies observed (Fig. 4c). In general, these hydrogels are soft ($G' = 0.5$ kPa at 1.5 wt% loading of HEC-Np) and display linear 'shear-thinning' behaviour, yet they are highly elastic ($\tan\delta \approx 0.3$). Moreover, the viscosity and mechanical properties can be easily tuned by simply altering the ratio of the polymers to CB[8] and their respective concentrations in solution.

Based on the storage modulus, G', the molecular weight between the effective crosslinks, M_c, was calculated according to equation (1) [29].

$$G' = \frac{\rho RT}{M_c} \tag{1}$$

where ρ is the polymer concentration (g m^{-3}), R is the molar gas constant, and T is the absolute temperature. The mesh size of the hydrogel is proportional to M_c and therefore a smaller M_c equates to a smaller mesh size [32]. M_c decreases from 190 kDa at lower HEC-Np concentrations (0.5 wt%) to 80 kDa at higher concentrations of HEC-Np (1.5 wt%) as the higher concentrations contain a higher packing of polymer chains. This direct correlation indicates that the hydrogel formulation can be tailored for specific control over the sustained release of protein therapeutics.

The microstructure of the hydrogels were characterized by scanning electron microscopy (SEM) and small-angle neutron scattering (SANS). Fig. 5 clearly shows a large dependence of the observed microstructure for two cryo-dried and lyophilized samples on the relative loading of HEC-Np and PVA-MV@CB[8]. Small-angle neutron scattering measurements on the hydrogels (HEC-Np 0.5%/PVA-MV 0.1%/CB[8] 1eq) were performed on the D11 instrument at the Institut Laue Langevin (ILL) (Grenoble, France). Scattering from hydrogels at higher loading was not measured on account of the impracticality of loading the material into the very

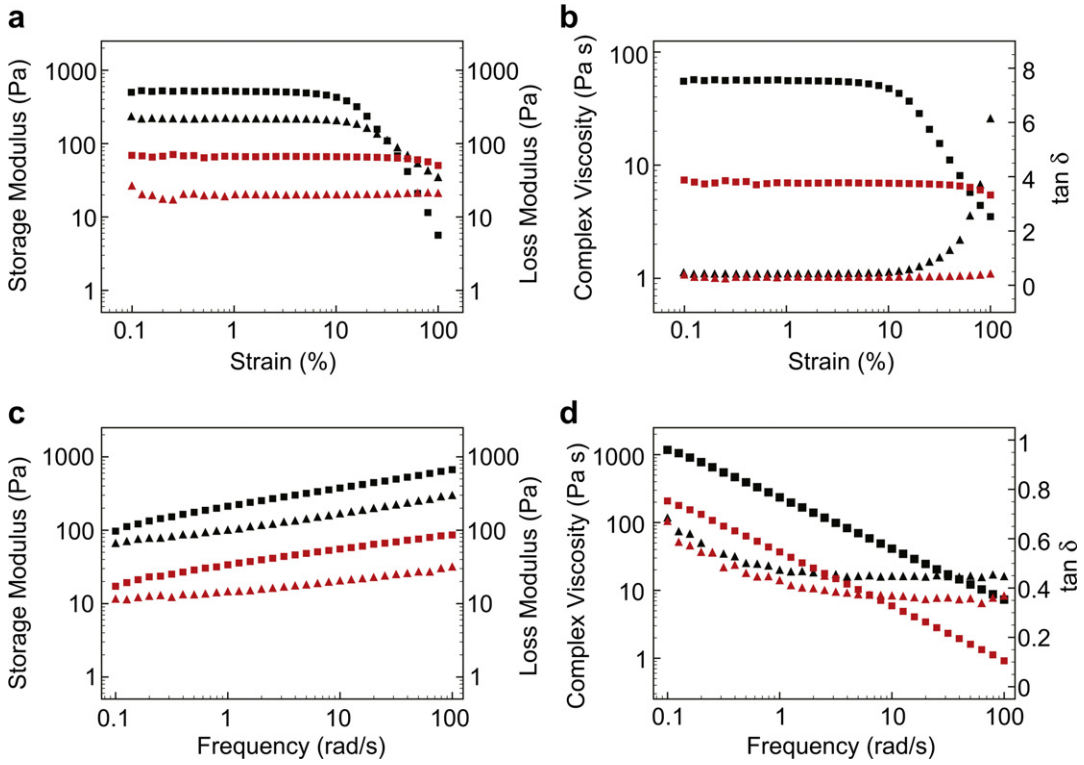

Fig. 4. Dynamic oscillatory rheological characterization performed at 37 °C of the HEC-based hydrogels used in this study. a, Storage and loss modulus and b, complex viscosity and tan δ taken from strain amplitude sweep measurements. c, Storage and loss modulus and d, complex viscosity and tan δ taken from frequency sweep measurements. Denotations are as follows: HEC-Np 1.5%/PVA-MV 0.3%/CB[8] 1eq (black) and HEC-Np 0.5%/PVA-MV 0.1%/CB[8] 1eq (red), whilst squares refer to the left axis and triangles to the right axis. (For interpretation of the references to colour in this figure legend, the reader is referred to the web version of this article.)

thin (1 mm) quartz cuvette. The data from higher q values can be appropriately described by a combination of the Debye-Bueche and Ornstein-Zerniche models [30,31]. The correlation length ξ could be fitted with values of 200 $\pm$ 30 Å, which is large compared to reported values for polymeric gels. The large value is likely on account of the exceptionally low loading of polymeric material relative to previously reported systems (typically $\geq$ 5 wt%), yet consistent with the calculated mesh size based on distances between guest moieties along an extended, well-solvated polymer chain. The correlation length of the frozen-in structure, Ξ, could take a wide range of values, between 500 and 1000 Å. A high excess scattering was observed at low q, which followed a q^{-4} Porod law, typical of a sharp interface, and suggesting the presence of very large size inhomogeneities in the sample. The scattering could therefore not be fully described by the Debye-Bueche and Ornstein-Zerniche models and a power law (q^{-4}) was needed to account for the full scattering curve. These inhomogeneities are likely resulting from insoluble pulp from the cellulose as the samples were not filtered before the scattering measurements were taken (Fig. 6).

In vitro cytotoxicity studies are of major importance when considering any biomedical application for such hydrogels and were performed using 3T3 fibroblast cells. These studies were performed using only the polymer constituents in order to maximize the availability to the cells and limit increases in viscosity due to hydrogel formation in the presence of CB[8]. A recent study of both *in vivo* and *in vitro* toxicity of cucurbit[*n*]urils has recently been performed which clearly demonstrates the biocompatibility and extremely low toxicity of these macrocyclic hosts [34]. The cytotoxicity of the polymers was tested at various concentrations ranging from 0.1 to 50 mg/mL and quantification of the cytotoxic response was done using an MTT assay. In general, the polymers do not show significant toxicity (Fig. 7). Additionally, the cytotoxicity of the leachable products from the copolymer gel was evaluated by incubating the gel in the cell culture medium over a period of 30 days at 37 °C to simulate usage conditions. Again, quantification of the cytotoxic response was done using the MTT assay. Aqueous extracts of the polymers do not show significant cytotoxicity against 3T3 cells. Our initial concerns were regarding the use of TDL

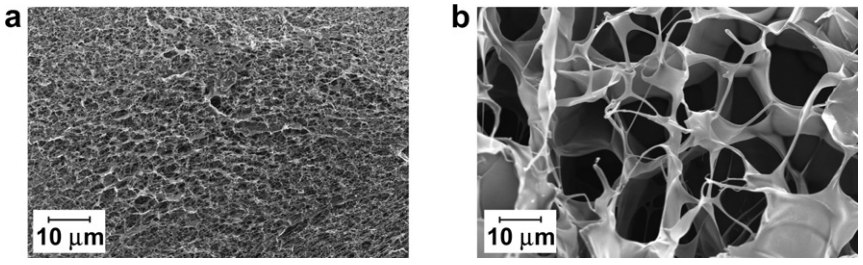

Fig. 5. Scanning electron microscopy images of a, HEC-Np 0.5%/PVA-MV 0.1%/CB[8] 1eq. b, HEC-Np 1.5%/PVA-MV 0.3%/CB[8] 1eq.

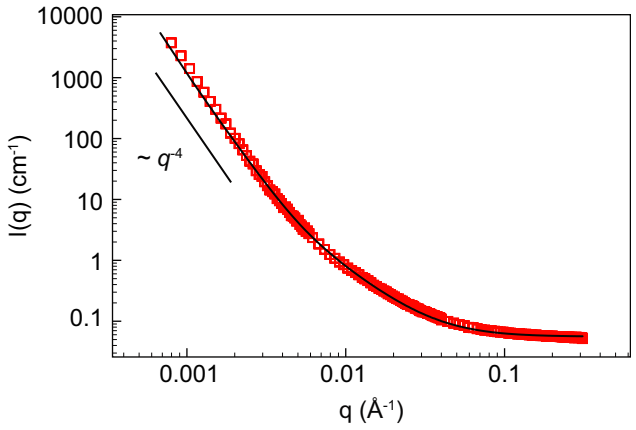

Fig. 6. Small-angle neutron scattering from HEC-Np 0.5%/PVA-MV 0.1%/CB[8] 1eq at 37 °C and associated theoretical fitting.

as a catalyst and the presence of the viologen moity, as both are known cytotoxic chemicals. However it has been shown that at very low concentrations (1 ppm), TDL did not elicit a cytotoxic response against the L929 mouse fibroblast cells [12]. From these studies, the polymeric constituents are not cytotoxic, highlighting that the viologen moiety is nontoxic when conjugated to a polymer backbone, and the resulting hydrogels are expected to be safe for biomedical applications.

3.2. Release studies of model protein therapeutics from supramolecular hydrogels

The low polymer concentration and high water content of this gel makes it highly attractive for biomedical applications due to improved biocompatibility. With the hydrogels in hand and appropriately characterized, several methods for the preparation of protein-loaded samples were investigated. Two model protein therapeutics were chosen for this study, Bovine Serum Albumen (BSA) and lysozyme, on account of their difference in size, providing information on the release of materials over a wide range of molecular sizes. As the hydrogels self-assemble rapidly at room temperature, it was possible to dissolve the protein with either of the polymeric solutions before mixing and *in situ* hydrogel formation. For this experiment, however, the proteins were encapsulated into the gels by admixing with preformed hydrogel. The protein-loaded gels were formed and then incubated at 37 °C and the release of the protein monitored over time. This form of protein loading method minimizes the risk of protein denaturation as it does not expose the protein to high heat or organic solvents during the formulation process. In this study, two factors affecting the protein release were studied, (1) the effect of total polymer concentration (0.5 wt% *versus* 1.5 wt%) and (2) the effect of protein molecular weights (BSA, M_w: 67,000 g mol^{-1} *versus* lysozyme, M_w: 14,000 g mol^{-1}).

The proteins were released in a continuous fashion and their release profiles are shown in Fig. 8. For all the curves except BSA-loaded 0.5 wt% gel, an initial burst release takes place before constant release is observed. When the polymer concentration is high, the rate of protein release is reduced and a more sustained release is observed. The burst release of the 0.5 wt% gel released approximately 50% of the BSA protein within the first 1 week whereas the 1.5 wt% gel managed to suppress this effect to approximately 10%. Moreover, BSA is a protein with a molecular weight of about 67,000 g mol^{-1} whereas lysozyme has a molecular weight of about 14,000 g mol^{-1} [32]. For BSA, the rate of release of the protein is slower when compared with lysozyme and a more sustained release is observed. The burst release is also effectively suppressed and the duration of sustained release is extremely promising. Previously, a sustained protein release profile of up to 80 days was demonstrated by the poly(PEG/PPG/PHB urethane) thermogels (formed at 5 wt% polymer constituents) reported by Loh *et al.* [12]. When the protein is large, the rate of release becomes correspondingly slower as the mobility of the protein out of the gel is reduced. The release profile of all the polymers can be fitted to the following Ritger–Peppas equation (2) for drug release in the range of $M_t/M = 0.6$ [35,36].

$$\frac{M_t}{M_\infty} = kt^n \tag{2}$$

3.3. Protein bioactivity

The preservation of protein activity is of great importance for any biological application involving gels. The biological activity of both BSA and lysozyme materials upon delivery from the hydrogel are shown in Fig. 9. The evaluation was performed using well established activity assays. Control experiments were performed whereby the proteins were kept in buffered solutions for the analogous time frames as the delivery. It is observed that BSA retains over 80% of its original activity when released from the gel even after 50 days, while 2% of the activity is retained after only 6 days without any gel encapsulation. These results imply that BSA maintains most of its activity when retained within the gel

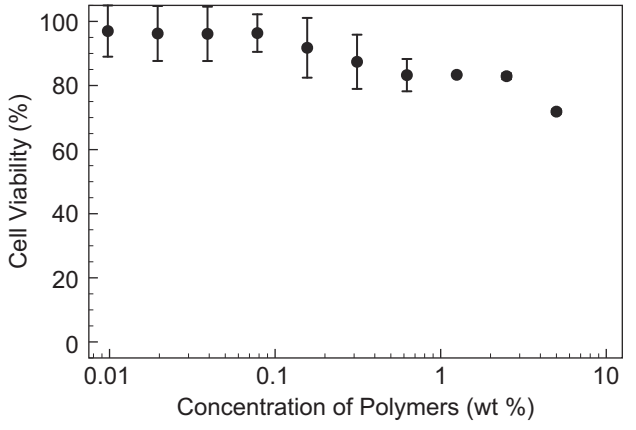

Fig. 7. Toxicity of the hydrogel constituent polymers HEC-Np and PVA-MV to 3T3 cells.

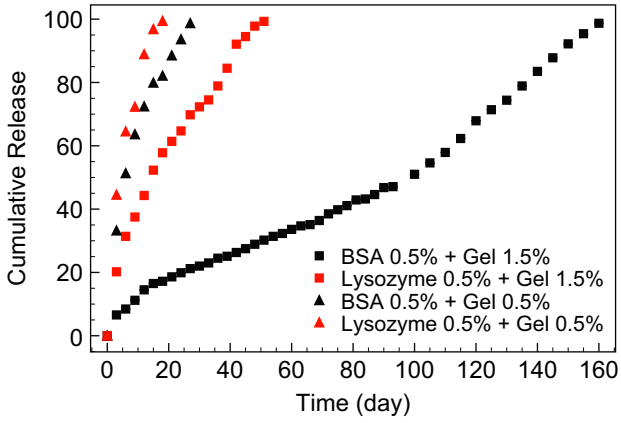

Fig. 8. Cumulative release of both BSA and lysozyme (0.5 wt%) from hydrogels formed at two levels of polymer loading (1.5 wt% and 0.5 wt%).

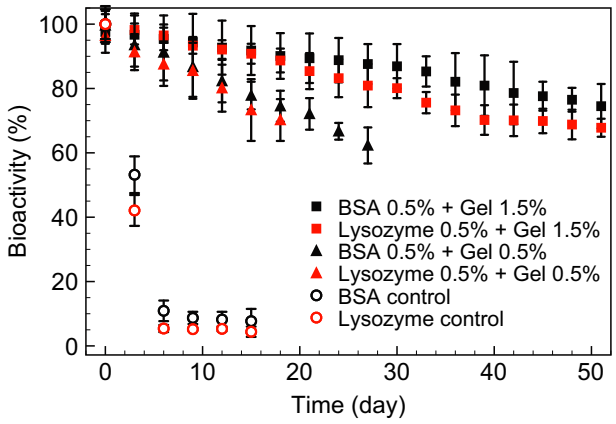

Fig. 9. Bioactivity of both BSA and lysozyme upon release from hydrogels formed at two levels of polymer loading (1.5 wt% and 0.5 wt%).

structure, which is likely a reflection of the retention of the native structure by BSA.

4. Conclusion

Self-assembled hydrogels with extremely high water content (up to 99.7%), highly tunable mechanical properties, biocompatibility have been prepared and the simplicity of their preparation at biologically relevant temperatures is distinguishing for important biomedical applications. The protein release characteristics of these self-assembled hydrogels were investigated and the correlation between the protein release of the polymer loadings of the hydrogels were studied. In the protein release studies, we observed that the gels released the entire loaded model protein. A short 'burst' release was observed in the initial stage of the drug release before a highly sustained, yet tuneable, diffusion-controlled release. This sustained release far surpassed the current state of the art for protein release from a hydrogel, highlighting these materials as important potential candidates for sustained therapeutic applications.

Appendix A. Supplementary material

Supplementary material associated with this article can be found, in the online version, at doi:10.1016/j.biomaterials.2012.02.030.

References

[1] Leader B, Baca QJ, Golan DE. Protein therapeutics: a summary and pharacological classification. Nat Rev Drug Disc 2008;7:21–39.
[2] Wu X, Yang Z-Y, Li Y, Hogerkorp C-M, Schief WR, Seaman MS, et al. Rational design of envelope identifies broadly neutralizing human monoclonal antibodies to HIV-1. Science 2010;329:856–61.
[3] Zhou T, Georgiev I, Wu X, Yang Z-Y, Dai K, Finzi A, et al. Structural basis for broad and potent neutralization of hiv-1 by antibody VRC01. Science 2010; 329:811–7.
[4] Miller NH. Compliance with treatment regimens in chronic asymptomatic diseases. Am J Med 1997;102:43–9.
[5] Lutolf MP. Spotlight on hydrogels. Nat Mat 2009;8:451–3.
[6] Staats HF, Leong KW. Chaperoning vaccines. Nat Mat 2010;9:537–8.
[7] Nochi T, Yuki Y, Takahashi H, Sawada S-i, Mejima M, Kohda T, et al. Nanogel antigenic protein-delivery system for adjuvant-free intranasal vaccines. Nat Mat 2010;9:572–8.
[8] Loh XJ, Peh P, Liao S, Sng C, Li J. Controlled drug release from biodegradable thermoresponsive physical hydrogel nanofibers. J Control Release 2010;143: 175–82.
[9] Loh XJ, Goh SH, Li J. Biodegradable thermogelling poly[(r)-3-hydroxybutyrate]-based block copolymers: micellization, gelation, and cytotoxicity and cell culter studies. J Phys Chem B 2009;113:11822–30.
[10] Loh XJ, Tan YX, Li Z, Teo LS, Goh SH, Li J. Biodegradable thermogelling poly(ester urethane)s consisting of poly(lactic acid): thermodynamics of micellization and hydrolytic degradation. Biomaterials 2008;29:2164–72.
[11] Loh XJ, Sng KBC, Li J. Synthesis and water-swelling of thermo-responsive poly(ester urethane)s containing poly(eta-caprolactone), poly(ethylene glycol) and poly(propylene glycol). Biomaterials 2008;29:3185–94.
[12] Loh XJ, Goh SH, Li J. Hydrolytic degradation and protein release studies of thermogelling polyurethane copolymers consisting of poly[(r)-3-hydroxybutyrate], poly(ethylene glycol), and poly(propylene glycol). Biomaterials 2007;28:4113–23.
[13] Li X, Loh XJ, Wang K, He C, Li J. Poly(ester urethane)s consisting of poly[(r)-3-hydroxybutyrate] and poly(ethylene glycol) as candidate biomaterials: characterization and mechanical property study. Biomacromolecules 2005;6: 2740–7.
[14] Silva AKA, Richard C, Bessodes M, Scherman D, Merten O-W. Growth factor delivery approaches in hydrogels. Biomacromolecules 2009;10:9–18.
[15] Tabata Y. The importance of drug delivery in tissue engineering. Pharm Sci Technol Today 2000;3:80–9.
[16] Esposito E, Carotta V, Scabbia A, Trombelli L, Dantona P, Menegatti E, et al. Comparative analysis of tetracycline-containing dental gels: poloxamer- and monoglyceride-based formulations. Int J Pharm 1996;142:9–23.
[17] Katakam M, Ravis WR, Golden DL, Banga AK. Controlled release of human growth hormone following subcutaneous administration in dogs. Int J Pharm 1997;152:53–8.
[18] Loh XJ, Goh SH, Li J. New biodegradable thermogelling copolymers having very low gelation concentrations. Biomacromolecules 2007;8:585–93.
[19] Appel EA, Biedermann F, Rauwald U, Jones ST, Zayed JM, Scherman OA. Supramolecular cross-linked networks via host–guest complexation with cucurbit[8]uril. J Am Chem Soc 2010;132:14251–60.
[20] Zhao N, Liu L, Biedermann F, Scherman OA. Binding studies on CB[6] with a series of 1-alkyl-3-methylimidazolium ionic liquids in an aqueous system. Chem-Asian J 2010;5:530–7.
[21] Marquez C, Hudgins RR, Nau WM. Mechanism of host-guest complexation by cucurbituril. J Am Chem Soc 2004;126:5806–16.
[22] Lagona J, Mukhopadhyay P, Chakrabarti S, Isaacs L. The cucurbit[n]uril family. Angew Chem Int Edit 2005;44:4844–70.
[23] Liu S, Ruspic C, Mukhopadhyay P, Chakrabarti S, Zavalij P, Isaacs L. The cucurbit[n]uril family: prime components for self-sorting systems. J Am Chem Soc 2005;127:15959–67.
[24] Kim J, Jung IS, Kim SY, Lee E, Kang JK, Sakamoto S, et al. New cucurbituril homologues: syntheses, isolation, characterization, and x-ray crystal structures of cucurbit[n]uril (n = 5, 7, and 8). J Am Chem Soc 2000;122: 540–1.
[25] Rauwald U, Biedermann F, Deroo S, Robinson CV, Scherman OA. Correlating solution binding and ESI-MS stabilities by incorporating solvation effects in a confined cucurbit[8]uril system. J Phys Chem B 2010;114:8606–15.
[26] Richard D, Ferrand M, Kearley GJ. Analysis and visualisation of neutron–scattering data. J Neutron Res 1996;4:33–9.
[27] Biedermann F, Appel EA, del Barrio J, Gruendling T, Barner-Kowollik C, Scherman OA. Postpolymerization modification of hydroxyl-functionalized polymers with isocyanates. Macromolecules 2011;44:4828–35.
[28] Kim J, Jung IS, Kim SY, Lee E, Kang JK, Sakamoto S, et al. New Cucurbituril Homologues: syntheses, isolation, characterization, and X-ray crystal structures of cucurbit[n]uril (n = 5, 7, and 8). J Am Chem Soc 2000;122:540–1.
[29] Goodwin JW, Hughes RW. Rheology for Chemists: an Introduction. Cambridge: The Royal Society of Chemistry; 2000.
[30] Benguigui L, Boue F. Homogeneous and inhomogeneous polyacrylamide gels as observed by small angle neutron scattering: a connection with elastic properties. Euro Phys J B 1999;11:439–44.
[31] Horkay F, Basser PJ, Hecht AM, Geissler E. Structural investigations of a neutralized polyelectrolyte gel and an associating neutral hydrogel. Polymer 2005;46:4242–7.
[32] Loh XJ, Nguyen VPN, Kuo N, Li J. Encapsulation of basic fibroblast growth factor in thermogelling copolymers preserves its bioactivity. J Mater Chem 2011;21:2246–54.
[33] Shioiri T, Kunihiro N, Shunichi Y. Diphenylphosphoryl azide. New convenient reagent for a modified curtius reaction and for peptide synthesis. J Am Chem Soc 1972;94:6203–5.
[34] Uzunova VD, Cullinane C, Brix K, Nau WM, Day AI. Toxicity of cucurbit[7]uril and cucurbit[8]uril: an exploratory in vitro and in vivo study. Org Biomol Chem 2010;8:2037–42.
[35] Ritger PL, Peppas NA. A simple equation for description of solute release I. Fickian and non-Fickian release from non-swellable devices in the form of slabs, spheres, cylinders or disks. J Control Release 1987;5:23–36.
[36] Ritger PL, Peppas NA. A simple equation for description of solute release II. Fickian and anomalous release from swellable devices. J Control Release 1987; 5:37–42.